J Ind Microbiol Biotechnol (2009) 36:971–979
DOI 10.1007/s10295-009-0576-1

ORIGINAL PAPER

Laboratory-scale biofiltration of acrylonitrile by *Rhodococcus rhodochrous* DAP 96622 in a trickling bed bioreactor

Jie Zhang · George E. Pierce

Received: 13 January 2009 / Accepted: 5 April 2009 / Published online: 22 April 2009

Abstract Acrylonitrile (ACN), a volatile component of the waste generated during the production of acrylamide, also is often associated with aromatic contaminants such as toluene and styrene. Biofiltration, considered an effective technique for the treatment of volatile hydrocarbons, has not been used to treat volatile nitriles. An experimental laboratory-scale trickling bed bioreactor using cells of *Rhodococcus rhodochrous* DAP 96622 supported on granular activated carbon (GAC) was developed and evaluated to assess the ability of biofiltration to treat ACN. In addition to following the course of treatability of ACN, kinetics of ACN biodegradation during both recycle batch and open modes of operation by immobilized and free cells were evaluated. For fed-batch mode bioreactor with immobilized cells, almost complete ACN removal (>95%) was achieved at a flow rate of 0.1 μl/min ACN and 0.8 μl/min toluene (TOL) (for comparative purposes this is equivalent to 6.9 mg l^{-1} h^{-1} ACN and 83.52 mg l^{-1} h^{-1} TOL). In a single-pass mode bioreactor with immobilized cells, at ACN inlet loads of 100–200 mg l^{-1} h^{-1} and TOL inlet load of ~400 mg l^{-1} h^{-1}, with empty bed retention time (EBRT) of 8 min, ACN removal efficiency was ~90%. The three-dimensional structure and characteristics of the biofilm were investigated using confocal scanning laser microscopy (CSLM). CLSM images revealed a robust and heterogeneous biofilm, with microcolonies interspersed with voids and channels. Analysis of the precise measurement of biofilm characteristics using COMSTAT® agreed with the assumption that both biomass and biofilm thickness increased along the carbon column depth.

J. Zhang · G. E. Pierce (✉)
Department of Biology, Georgia State University,
Atlanta, GA, USA
e-mail: biogep@langate.gsu.edu; gpierce@gsu.edu

Keywords *Rhodococcus* · Acrylonitrile · Wastewater treatment · Trickling bed bioreactor

Introduction

Acrylonitrile (ACN) is an important raw material and chemical intermediate used in the production of acrylic fibers, plastics and synthetic rubber, and is used in the preparation of solvents, pharmaceuticals and insecticides [25]. ACN, a colorless, liquid, synthetic chemical, is partially soluble in water (7 g/100 ml at 20°C) and evaporates quickly [1]. Of all the commercial nitriles, ACN is manufactured on the largest scale. Adverse effects of ACN on human health and the environment are well documented [4, 7, 24, 26, 31]. The current US EPA recommendation for ACN in lakes and streams is <0.058 ppb to prevent possible health effects [1]. Given these concerns, ACN manufacturing industries are required to reduce primarily the organic load from their discharges [23]. In 1996 approximately 80 plants in 22 countries produced 4.3 million tons of ACN [28]. Global annual production of ACN in 2001 was 3.9 million tons, and in 2005, 5.9 million tons, with just under half of that coming from the United States.

Currently, deep well injection disposal technology and wet air oxidation are used to address ACN contaminated wastewaters. These two technologies in addition to being costly also have the potential to generate secondary air or water pollution. Biofilter and biotrickling filters have increasingly become methods of choice for treating gaseous and vapor-phase organic contaminants in air streams or present in wastewaters. While there are considerable references that support the use of biotrickling filters to remove organic pollutants in contaminated air and water

[2, 5, 8, 19, 20, 32], research with biofilter and biotrickling filter has not addressed ACN biodegradation.

Granular activated carbon (GAC) serves as a good initial substratum candidate for bacterial immobilization because relatively large spaces between granules allow liquids to trickle down freely while gas flow is unrestricted through either a packed or expended bed. Bacterial reactors using GAC as a support have been investigated for the biotreatment of numerous organics including aromatic hydrocarbons such as benzene, toluene, xylene and chlorobenzene, as well as phenol and 4-chlorophenol [11, 15, 21, 30]. The bioconversion of nitrile to the corresponding amide and acid salt through the action of nitrile hydratase (NHase) and amidase by *Rhodococcus rhodochrous* is well documented [12, 18, 27, 29]. However, the application of *Rhodococcus* or similar ACN degrading bacteria to treat ACN in a trickling filter system has not been reported.

This study examines the conditions at the laboratory scale that result in the retention and maintenance of viable *R. rhodochrous* cells possessing highly active NHase and amidase activity, and the kinetics of ACN biodegradation in a model trickling bed bioreactor under both recycle batch conditions and single-pass system. For this purpose, a laboratory-scale trickling bed bioreactor was constructed, and the biofiltration performance was evaluated and the biofilm properties in the reactor were characterized.

Methods

Microorganism

Rhodococcus rhodochrous DAP 96622 (ATCC 55898) was obtained from American Type Culture Collection (Vienna, VA) and was maintained either on yeast extract malt extract medium (YEMEA) [9] or Stanier's minimal medium [22] supplemented with 5 g l^{-1} glucose and 1 g l^{-1} ammonia sulfate. Working cultures of DAP 96622 were first grown in the supplemented Stanier's medium and subsequently adapted to increasing ACN concentrations up to about 500 mg l^{-1} and toluene (TOL) concentrations up to 1,000 mg l^{-1}, as additional compounds to the supplemented medium. The fully adapted DAP 96622 culture was used as the inoculum for degradation kinetic studies and for the reactor start-up.

Laboratory-scale reactor

For the laboratory-scale trickling bed reactor, a Chromoflex® Plexiglas column (19 cm length × 5.5 cm i.d.) (Kontes, Vineland, NJ) was filled with 60 g of granular activated carbon (Calgon Filtersorb F-300 Grade, Pittsburgh, PA) providing a total working volume of 190 ml (bed volume 130 ml and void volume 60 ml, with 6.2 cm bed height) (Fig. 1). Liquid medium was continuously fed with a peristaltic pump (model EW-07521-50, Masterflex L/S; Cole-Parmer, Vernon Hills, IL) at 1 ml/min through the top of the reactor and allowed to trickle down by gravity. Ambient air was bubbled through the buffer solution in the influent tank (at 2 l/min) and the buffer tank (at 0.15 l/min), under the control of a mass flow meter (GFM 37, Aalborg, NY) with an air pump [Gast (model DOA-V722-AA, Benton Harbor, MI)]. Aerated buffer was pumped to the influent tank and then to the top of the reactor with a peristaltic pump (model EW-07543-30, Masterflex L/S; Cole-Parmer, Vernon Hills, IL). ACN and TOL were added to the liquid influent just prior to the liquid entering the reactor via syringe pump (Model 22, Harvard Apparatus, Holliston, MA). Dissolved oxygen (DO) concentrations in the influent and effluent tanks were measured by polarographic DO probes (Ingold model 4300; Mettler-Toledo, Wilmington, MA). The DO concentration in the influent tanks was maintained above 6 mg l^{-1}. A VOC trap (40 cm length × 0.8 mm i.d. containing 5 g of VOC grade GAC) was connected to the top of the column to adsorb escaped organics.

Batch mode bioreactor

Batch studies were carried out under aerobic conditions using *R. rhodococcus* DAP 96622 previously adapted to

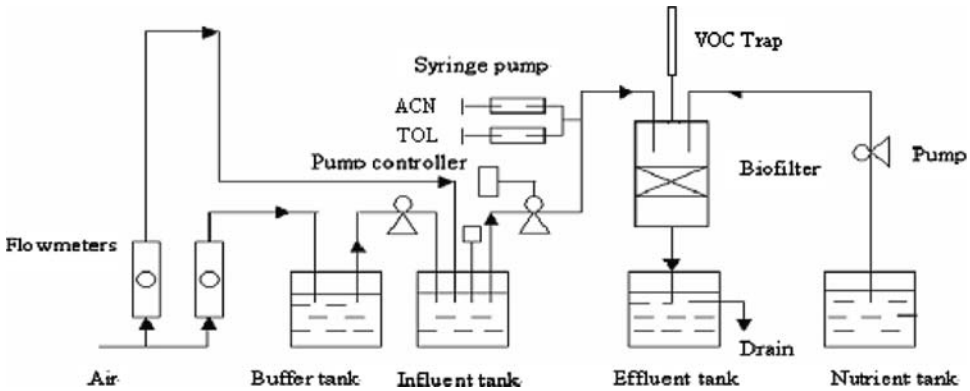

Fig. 1 Schematic representation of the experimental set-up

ACN and TOL at 500 and 1,000 mg l^{-1}, respectively. A 20-ml cell suspension (containing 50 mg packed wet weight cells) was introduced into the reactor, and the flow was continuously recycled with Stanier's medium containing an initial fed ACN and TOL concentration of ~300 and ~1,000 mg l^{-1}, respectively, for a month. We added TOL at 1,000 mg l^{-1} to provide a reservoir (saturation) in the reactor systems. Total recycled liquid was 500 ml. Optical density (OD) of cells and ACN and TOL concentrations in the reservoir were measured periodically over 15 days. ACN/TOL bound to the trap was estimated after extraction. The charcoal in the column was assumed to be saturated with ACN/TOL at steady state.

Kinetic studies

Cells of ACN/TOL adapted *Rhodooccus* DAP 96622 were investigated for their ability to degrade ACN in both flasks and in the bioreactor. Erlenmeyer flasks (125 ml) containing 30 ml Stanier's medium to which 0.3 mg cobalt and 0.225 g urea were added were supplemented with ACN at 100–1,000 mg l^{-1}. A 5 ml cell suspension made from 7-day culture pre-grown on Stanier's agar with ACN, and TOL was added to each flask to an OD_{600} of 0.6. Uninoculated flasks served as a control to correct for abiotic loss of ACN and TOL. For the bioreactor with GAC-associated-immobilized cells, ACN and TOL were injected to the recycle bottle from stock solutions to give various substrate concentrations, starting from low to subsequently high concentrations. Liquid samples were periodically withdrawn to measure OD and ACN concentrations. The degradation rate was estimated from the initial or maximum slope of the concentration curve, and the specific growth rate was obtained from the slope of the semi logarithmic plot of OD versus time. Fresh substrate was added when the substrate in the reservoir was depleted.

Biofiltration study

When the biofilter showed a high removal efficiency of ACN and TOL and reached steady state, it was shifted from liquid-continuous mode (with refeeding) to single-pass mode. ACN and TOL were added to aerated buffer, which was then trickled down the bed from the top at a rate of 1 ml/min. The reactor performance under steady-state conditions with ACN as the single feed was also evaluated. Under these conditions, ACN flow rate to the reactor was gradually increased from 0.2 to 1.0 μl/min.

Experimental results were expressed in terms of the ACN inlet load (IL) (mg l^{-1} h^{-1}), the elimination capacity (EC) (mg l^{-1} h^{-1}), and the biofilter removal efficiency (RE) (%). These process parameters were calculated according to equations below:

$$\text{Empty bed retention time (EBRT)} = \text{Bed void volume}/Q$$

$$\text{ACN inlet load (IL)} = \text{QC}_{\text{in}}/V \text{ or } C_{\text{in}}/\text{EBRT}$$

$$\text{Removal efficiency (RE)} = (1 - C_{\text{out}}/C_{\text{in}}) * 100\%$$

$$\text{E lim ination capacity (EC)} = Q\,(C_{\text{in}} - C_{\text{out}})/V$$

where C_{in} was the inlet concentration of the organics (mg l^{-1}) and C_{out} was the outlet concentration of the organics (mg l^{-1}). Q was the liquid flow rate, and V was the volume of the filter bed (ml).

Analytical procedures

ACN and TOL were extracted from the medium with methylene chloride-methanol [85:15 (v/v)] based on EPA method 8031[10]. Extracts were analyzed by gas chromatography (HP5890, series II, Palo Alto, CA) equipped with a fused silica megabore column (75 m in length, 0.53 mm i.d., 3-μm film; DB-624, Agilent-J&W, Palo Alto, CA) and a flame ionization detector. Helium was used as the carrier gas at a flow rate of 18 ml/min. The temperature for column, injector and detector were 300, 300 and 250°C, respectively. For the sample, 0.5 μl from the extraction was injected with a liquid tight microsyringe (Agilent 5181-1273). The detection limits for ACN and TOL were 1 mg l^{-1} and 0.5 mg l^{-1}, respectively.

Confocal laser scanning microscopy

After 50 days in the single-pass mode, individual GAC particles were removed from the reactor column and stained with acridine orange, 0.005 (w/v) in phosphate buffer (pH 7.2). Images of biofilms were generated by CLSM (Zeiss LSM510 Confocal Microscope, Carl Zeiss Inc., Thornwood, NY). The pinhole was set to 108 μm, and excitation was obtained at 488 nm. Sampling of the fluorochrome was achieved with a LP505 filter. Samples were examined in both horizontal (x,y) and sagittal (x,z) planes as optically thin sections (1.0–1.1 μm) and images analyzed by COMSTAT (MATLAB 5.3, The Math Works Inc., Natick, MA).

Results

Kinetics studies of planktonic cells: i.e., cells suspended in the broth in the flasks and the GAC-associated-immobilized cells in the bioreactor

The effects of ACN concentration on ACN degradation rate and specific growth rate of planktonic cells (free cells in suspension) of adapted DAP 96622 grown on ACN in flasks

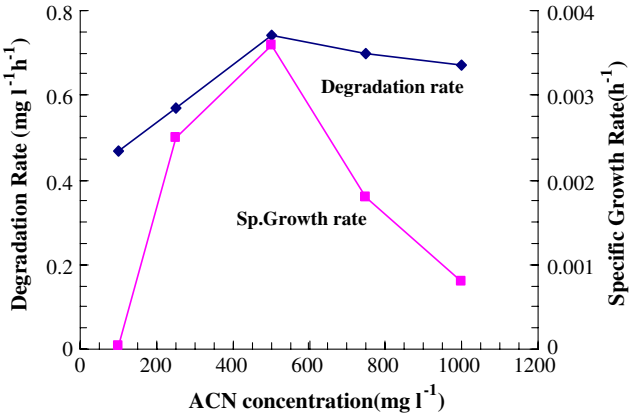

Fig. 2 Effect of ACN substrate concentration on degradation rate and specific growth rate of *Rhodococcus* DAP 96622 planktonic cells grown on ACN in flasks

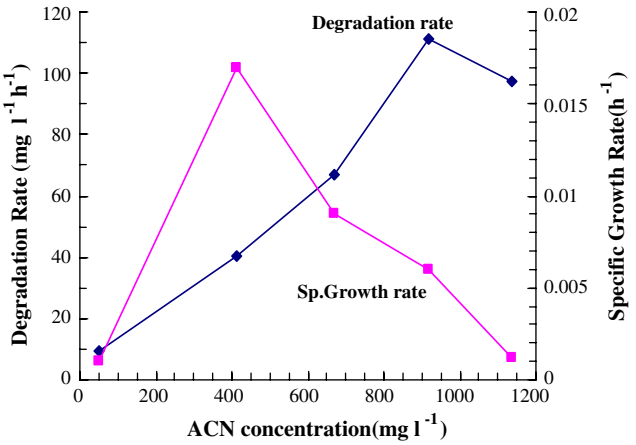

Fig. 3 Effect of ACN concentration on growth rate and degradation rate of ACN by *Rhodococcus* DAP 96622 immobilized cells in the feed-batch mode carbon-bed bioreactor (with toluene present at 1,000 mg l^{-1})

are shown in Fig. 2. Both growth rate and biodegradation rate increased with increasing ACN concentration up to 500 mg l^{-1} and then decreased. The adverse effect of ACN above 500 mg l^{-1} was more pronounced with respect to cell growth than to biodegradation.

In the presence of TOL, ACN adapted cells of DAP 96622 (GAC-associated immobilized cells) degraded significantly higher concentrations of ACN and yielded a larger biomass than planktonic cells in a batch culture with similar substrate concentration (compare Figs. 2, 3). In the batch-mode trickling bed bioreactor with toluene present (ACN:TOL = 1:2), the maximum growth and ACN degradation rate were 0.019 h^{-1} and 115 mg l^{-1} h^{-1}, respectively, for GAC-associated (immobilized) cells, compared with 0.0035 h^{-1} and 0.75 mg l^{-1} h^{-1} for planktonic cells.

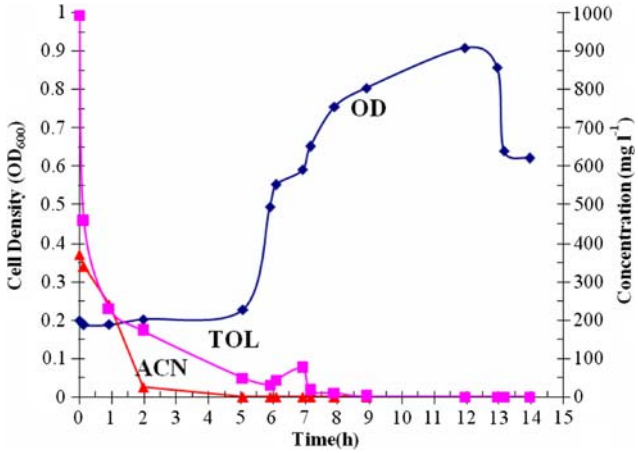

Fig. 4 Cell density profile, and ACN and TOL degradation in batch-mode reactor with liquid recycle. (◆) OD; (■): TOL concentration. (▲) ACN concentration. The mixtures of ACN and TOL were supplied continuously to the top of the column for ~12 days. The liquid empty bed retention time (EBRT, bed volume/liquid flow rate) was set for 6 min, and the bioreactor reached steady state after 2 days

Table 1 ACN and TOL removal efficiency with different flow rates of ACN and toluene in fed-batch-mode bioreactor[a,b]

Flow rate		ACN removal (%)	TOL removal (%)
ACN (μl/min)	TOL (μl/min)		
1	0	90–98	–
0.4	0.4	80–90	90–99
0.8	0.8	72–82	93–100
0.1	0.8	95–100	94–98

[a] Total liquid volume = 500 ml

[b] Column bed void volume = 60 ml

Batch mode bioreactor

During the start-up of the batch mode (liquid-recycle) operation, there was an initial lag of 6 days before the cell density began to increase, after which cell density in the reservoir continued to increase exponentially up to day 12. Total liquid volume recycled through the column was 500 ml. The OD was determined from cell density in the liquid sample taken from the reservoir during the recycle mode. Both ACN and TOL in the liquid were depleted after 5 and 9 days, respectively, prior to exponential cell growth (Fig. 4). Growth continued for an additional 4 days after TOL was no longer detected in the recirculation liquid. From this, it was assumed that the small portion of ACN and TOL that could have been absorbed by the activated carbon was bioavailable and supported cellular growth.

Almost complete ACN removal (>95%) was achieved at an organic load of 0.1 μl/min ACN and 0.8 μl/min TOL (0.32 g ACN l^{-1} day^{-1} and 2 g TOL l^{-1} day^{-1}) (Table 1).

The reactor efficiency for ACN decreased to below 80% when the ACN load was increased to 0.8 µl/min (while TOL load remained unchanged).

Single-pass open mode reactor

Reactor performance at steady-state: effects of inlet load on removal efficiency

At ACN inlet loads of 100–200 mg l^{-1} h^{-1} and at an EBRT = 4 min, removal efficiencies of greater than 90% were achieved (Figs. 5, 6). TOL removal efficiency of more than 80% was maintained at TOL loads of 400 mg l^{-1} h^{-1} at EBRT = 8 min, while only 50% removal efficiency could be achieved at the same TOL loading at an EBRT = 4 min (Fig. 6). It is noted that the transformations of ACN to acrylamide and subsequently to acrylic acid and ammonia are hydrolysis reactions, and thus indifferent to D.O., whereas TOL degradation requires oxygen, and it is therefore influenced by D.O. Compared with ACN, TOL removal efficiency was more sensitive to EBRT and to oxygen (Fig. 7).

Reactor performance at steady-state: effects of EBRT on removal efficiency

Maximum ACN removal efficiency of 85% was obtained at an ACN/TOL flow rate of 0.1 and 0.8 µl/min at an EBRT = 8 min, respectively. At the same EBRT (8 min),

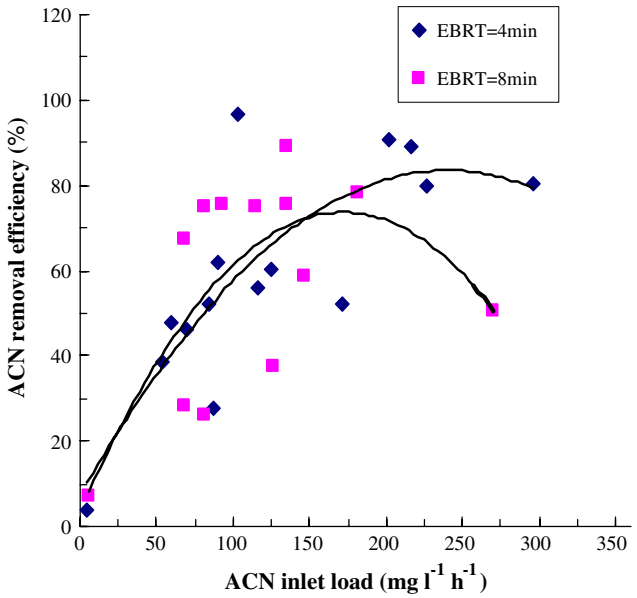

Fig. 5 Effect of ACN inlet load on ACN removal efficiency while maintaining a constant EBRT of 4 min or 8 min (flow rate ACN 0.1 µl/min TOL 0.8 µl/min). (Curve: polynomial. Statistical difference is not evident)

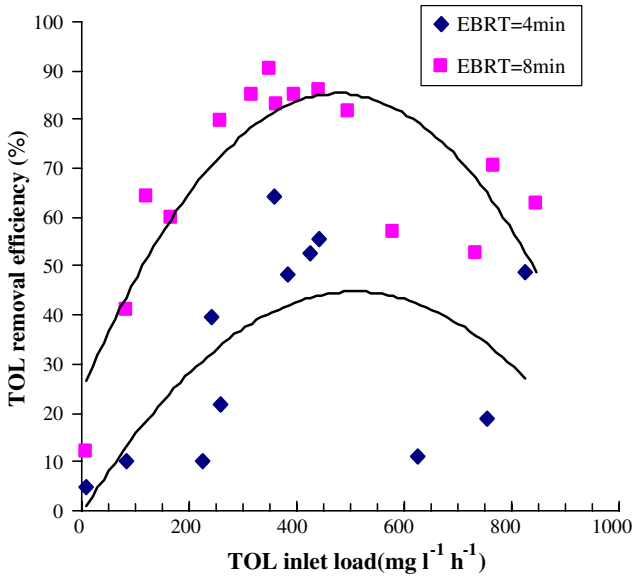

Fig. 6 Effect of TOL inlet load on TOL removal efficiency while maintaining a constant EBRT of 4 min or 8 min (flow rate ACN 0.1 µl/min TOL 0.8 µl/min)

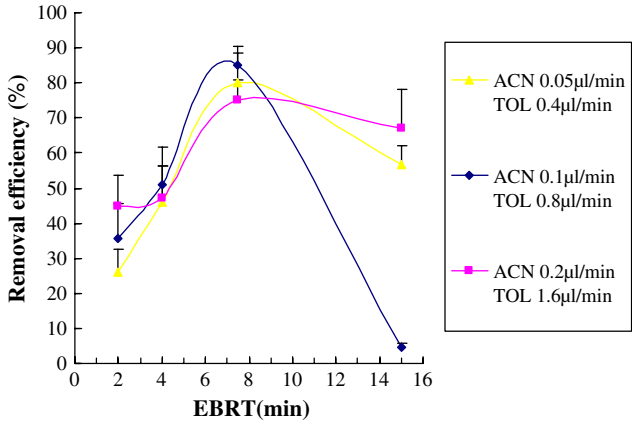

Fig. 7 Effects of EBRT on ACN removal efficiency at different ACN and TOL flow rates. ACN and TOL were introduced from the syringe pump to the top of the biofilter at flow rate of 0.05 µl/min ACN and 0.4 µl/min TOL, 0.1 µl/min ACN and 0.8 µl/min TOL, 0.2 µl/min ACN and 1.6 µl/min TOL, respectively. The data are average values from measurements collected after the biofilter reached pseudo-steady state at each specific condition

at flow rates between 0.05 µl/min ACN with 0.4 µl/min TOL, and 0.2 µl/min ACN with 1.6 µl/min TOL, removal efficiency was more than 70%. At the high liquid flow rates both column flooding and bed clogging occurred due to the overgrowth of the biomass.

ACN as sole feed

The elimination capacity (EC) and removal efficiency (RE) as affected by inlet ACN concentration at EBRT = 8 min when ACN was the sole carbon source in open, single

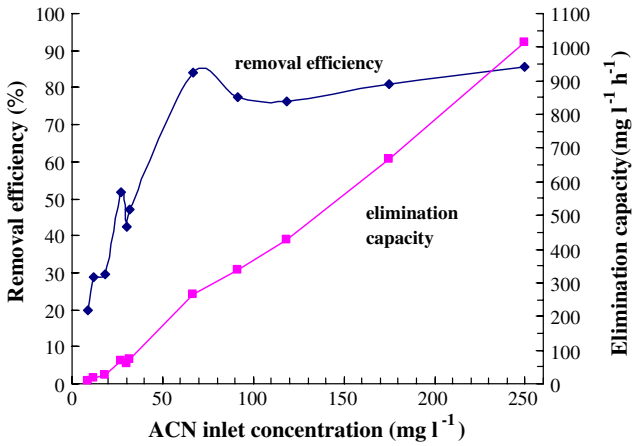

Fig. 8 ACN removal efficiency and elimination capacity versus ACN inlet concentration at EBRT = 8 min, with ACN as the sole carbon source

pass-mode operation reactor is shown in Fig. 8. From an ACN inlet concentration of 10–70 mg l^{-1}, RE increased rapidly with increasing inlet concentration. Above inlet concentration of 70, up to 250 mg l^{-1}, RE was relatively stable at between 75 and 85%. Throughout the ACN concentration range at 10–250 mg l^{-1}, EC increased steadily. At higher flow rates (EBRT < 4 min; data not shown), severe flooding and limited mass transfer between the gas-liquid phase and the biofilm occurred, which resulted in low ACN RE and EC.

Treatment kinetics for ACN as sole carbon source

NHase-mediated hydrolysis of ACN to acrylamide does not involve oxygen. The elimination capacity can be described by the following equation:

$$EC = (V_{max} \times C_{in})/(K_m + C_{in})$$

(V_{max}: the maximum degradation rate; K_m: half-saturation constant.)

The degradation rate can be first-order ($C_{in} \ll K_m$) or zero-order ($C_{in} \gg K_m$). Figure 9 shows that an EBRT of 8 min plot of inlet concentration versus elimination capacity can be fitted satisfactorily by linear regression when ACN was the single feed at EBRT = 8 min, indicating that the bioreaction follows first-order kinetics, and one cannot clearly distinguish between reaction and diffusion limited regimes. The following is based on the kinetics recently developed by Jin et al. (2006) [13]:

$$V_{max}/V = 1 + K_m/C$$

where $C = (C_{in} - C_{out})/\ln (C_{in}/C_{out})$

The relationship between substrate consumption rate and the mean log of inlet/outlet concentrations was expressed as $V = f(C)$. When C_{in} was plotted against C, a good-fit linear regression ($R^2 = 0.99$) was obtained.

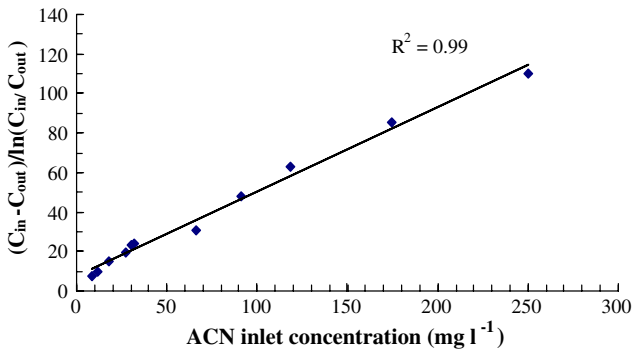

Fig. 9 ACN inlet concentration versus $(C_{in} - C_{out})/\ln (C_{in}/C_{out})$ when ACN was sole carbon and nitrogen source at EBRT = 8 min

Biofilm characterization

In the laboratory-scale reactors, a biofilm of ACN degrading microorganisms was present at all depths as scattered cells or clusters. CLSM images of the biofilm attached on GAC particles at the upper, middle and lower sections of the laboratory-scale reactor indicated a robust and heterogenerous biofilm, with an irregular distribution of microcolonies interspersed with voids and channels (Fig. 10). Characteristics of each section as quantified by the computer program COMSTAT are presented in Table 2. The roughness coefficient was highest for the upper section, and is likely caused by the formation and presence of elongated cell clusters and long filaments, whereas the roughness was lower for the lower section, a possible result of a limited supply of nutrients. The surface-volume ratio was relatively higher for upper and middle sections, because they had better access to the limited supply of nutrients. CLSM analysis also revealed a channeling structure partially filled with extracellular polymeric substances (EPS) for the upper and middle sections as opposed to the lower section, which further supports the case for diminished biofilm growth in the lower section. Although this diminished growth in the lower section could be related to impedance of substrate diffusion, the porous nature of GAC packing reduces this possibility [14, 16].

Discussion

Cells of ACN-adapted *Rhodococcus rhodochrous* DAP 96622 when associated with a non-sterile, activated charcoal column with increased growth significantly reduced ACN concentrations in a bioreactor reservoir.

ACN-adapted immobilized cells in the bioreactor at starting concentrations of ACN up to 1,150 mg l^{-1} in the presence of TOL had 10- to 100-fold higher ACN degradation rates than those of planktonic cells in flasks. Also,

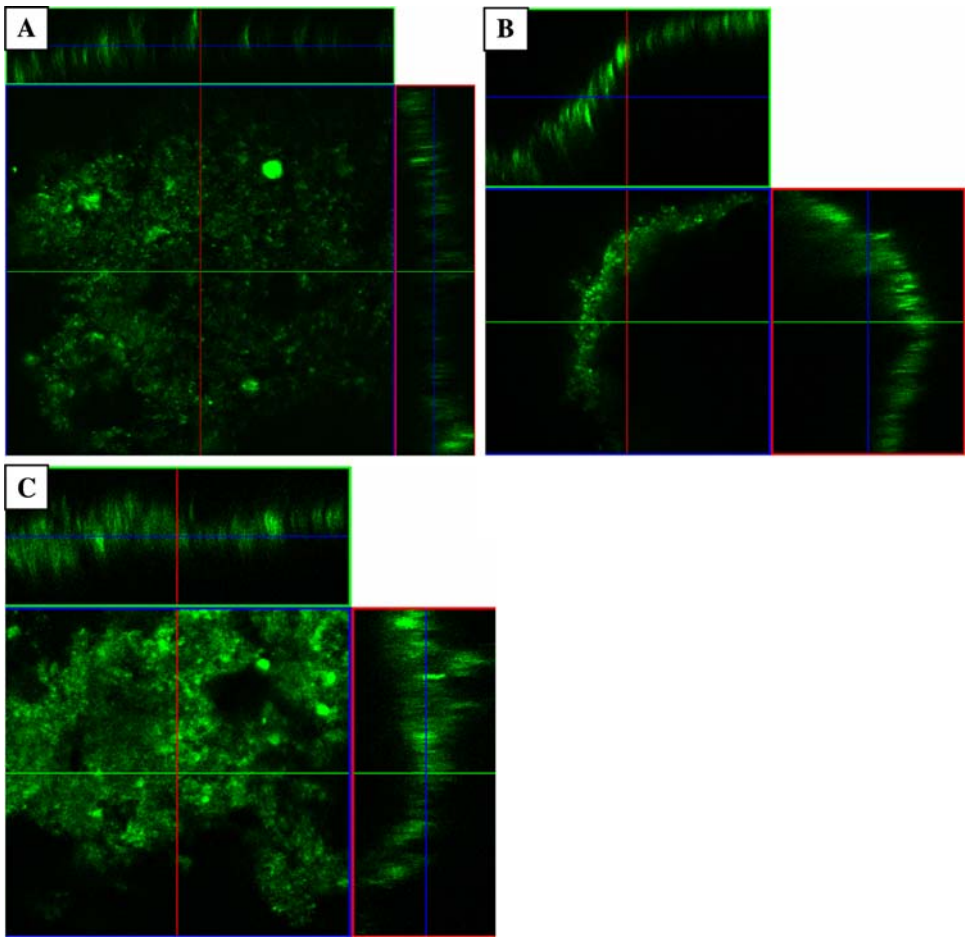

Fig. 10 CLSM images of biofilm attached to GAC particles, taken from upper (**a**), middle (**b**) and lower (**c**) parts of the reactor after 50 days in the single-pass mode. Magnification, ×400. *Red line*: axis *X*; *green line*: axis *Y*; *blue line*: axis *Z*

Table 2 Total biomass, average/maximum thickness, roughness, substratum coverage and surface to volume ratio of biofilms on GAC particles taken from the upper, middle and lower parts of the reactor (samples were taken at day 50)

	Upper section	Middle section	Lower section
Total biomass ($\mu m^3/\mu m^2$)	0.55 ± 0.05	3.20 ± 3.06	12.38 ± 0.16
Average thickness (μm)	2.12 ± 0.99	19.01 ± 11.08	43.24 ± 4.60
Maximum thickness (μm)	55.50 ± 19.09	98.00 ± 0.00	86.00 ± 2.83
Roughness coefficient	1.85 ± 0.00	1.38 ± 0.43	0.45 ± 0.03
Substratum coverage (%)	0.008 ± 0.006	0.017 ± 0.0095	0.03 ± 0.03
Surface to biovolume ratio ($\mu m^2/\mu m^3$)	26.16 ± 0.24	32.23 ± 13.28	19.52 ± 4.16

Values are means from two image stacks. The standard deviation is calculated as the square root of the mean of the variances of each of the two groups

GAC-associated cells were sensitive to ACN at significantly higher concentrations than planktonic cells. Furthermore, GAC-associated immobilized cells in the bioreactor tolerated and continued to degrade concentrations of ACN 1,150 mg l^{-1} at 95 mg l^{-1} h^{-1}, which were toxic for free cells. A near steady state of ACN degradation was maintained at 75-85% for ACN and 80%-90% for TOL within the parameter of EBRT = 8 min and ACN and TOL inlet loads between 50–200 mg l^{-1} h^{-1} and 200–500 mg l^{-1} h^{-1}, respectively. However, when the inlet load of ACN was increased to more than 200 and 500 mg l^{-1} h^{-1} for TOL, a reduction in efficiency (percentage) of ACN degradation was observed. The loss of efficiency was likely due to insufficient mass transfer within the biofilter and a decrease in the contact time between the influent and the microbes [3]. Furthermore, oxygen limitation at high concentrations and shorter EBRT may cause the reduction in efficiency. The addition of TOL addresses ACN sensitivity, but introduces mass transfer

issues at higher TOL because of oxygen requirements. The penetration depth of oxygen in aerobic biofilm reactors is often shallow (typically 100–150 μm) with near 50% of the oxygen consumed by the biofilm supplied by the channels [6].

Nagasawa et al. (1988) reported that nitrile hydratase activity of *Rhodococcus rhodochrous* J1 decreased with increasing nitrile concentration up to 70 g/l [17]. According to Haldane-Andrew's substrate inhibition equation:

$$\mu_g = \mu_{max} S/\left(K_S + S + S^2/K_i\right)$$

(μ_g: specific growth rate; μ_{max} :maximum specific growth rate; S: substrate concentration; K_S: substrate affinity constant; K_i: substrate inhibition constant)

Single substrate-limited microbial growth can be extended to the inhibition of microbial growth by high levels of substrates. Since in flasks ACN showed inhibition to cell growth, the equation could be used in modeling kinetics with high substrate concentrations. For immobilized cells, when the cell density in the bioreactor is relatively constant with respect to time, the substrate concentration rate can also be modeled by a similar equation.

In the ACN-degrading biofilms, microorganisms were present at all depths, either in dense cell clusters or as individuals. The formation of EPS, which binds bacteria together and enhances adhesion to surfaces, increased with time. A sagittal plane or stacks of slices revealed a network of channels either as long void spaces or filled with cells embedded on the EPS. Microorganisms not only colonized GAC carbon surfaces, but also the crevices, making a heterogeneous biofilm structure.

In our study, CLSM analysis also revealed a channeling structure partially filled with EPS.

Total biomass, average/maximum thickness, roughness, substratum coverage and surface-to-volume ratio suggested that the mix community biofilm had a stronger tendency to form micro-colonies and accumulated biomass in the deeper or lower sections (Fig. 10, Table 2). The gradual biomass accumulation in the lower zone may have ultimately caused channeling problems, leading to a reduced overall removal efficiency. This in part may be due to the supply system of the nutrient and buffer solution from the top displacing part of the biomass to the bottom. This maybe occurred during backwashing at a high flow rate with the following liquid drainage.

Conclusion

Rhodococcus in a laboratory-GAC bioreactor was adapted to efficient degradation of ACN + TOL under high inlet load/substrate concentration. Immobilized cells were less sensitive to combined ACN and TOL than planktonic cells and were capable of degrading ACN at ACN concentrations toxic for planktonic cells. When ACN was the single feed at an inlet concentration above 70 mg l^{-1}, removal efficiency was relatively stable at between 75-85%. *Rhodococcus* survived a fairly long period (>30 days) without nutrient addition to the filter bed, during which the filter bed was not loaded. The microbial activity was maintained in the moisturized bioreactor for 2 or 3 weeks.

Future studies of secondary processes that control *Rhodococcus* biomass in ACN reactor systems are warranted.

Acknowledgment We thank Dr. Gene Drago (Georgia State University) for helping set up the bioreaction system and Dr. Robert Simmons (Georgia State University) for the micrographs. The work was supported by Cytec Industries Inc. and the Georgia State University Research Foundation.

References

1. Agency for Toxic Substances and Disease Registry (ATSDR) (1999) Managing hazardous materials incidents. Volume III—Medical management guidelines for acute chemical exposures: acrylonitrile. US Department of Health and Human Services, Public Health Service, Atlanta, GA
2. Calderia M, Heald SC, Carvalho MF, Vasconcelos I, Bull AT, Castro PML (1999) 4-Chlorophenol degradation by a bacterial consortium: development of a granular activated carbon biofilm reactor. Appl Microbiol Biotechnol 52:722–729. doi:10.1007/s002530051584
3. Chang I, Gilbert E, Eliashberg N, Keasling JD (2003) A three-dimensional, stochastic simulation of biofilm growth and transport-related factors that affect structure. Microbiology 149:2859–2871. doi:10.1099/mic.0.26211-0
4. Collins JJ, Page LC, Caprossi JC, Utidjian HM, Saipher J (1989) Mortality patterns among employees exposed to acrylonitrile. J Occup Med 31:368–371. doi:10.1097/00043764-198907000-00013
5. Cox HHJ, Deshusses MA (2002) Effect of starvation on the performance and re-acclimation of biotrickling filters for air pollution control. Environ Sci Technol 36:3069–3073. doi:10.1021/es015693d
6. De Beer D, Stoodley P, Lewandowski Z (1994) Liquid flow in heterogeneous biofilms. Biotechnol Bioeng 44:636–641. doi:10.1002/bit.260440510
7. De Meester C, Poncelet F, Ropberfroid M, Mercier M (1978) Mutagenicity of acrylonitrile. Toxicology 11:19–27. doi:10.1016/S0300-483X(78)90239-1
8. Deshusses MA, Cox HHJ (1998) Biological waste air treatment in biotrickling filters. Curr Opin Biotechnol 9:256–262. doi:10.1016/S0958-1669(98)80056-6
9. Dietz A, Thayer DW (eds) (1980) Actinomycete taxonomy (procedures for studying aerobic actinomycetes with emphasis on the Streptomycetes). Society for industrial microbiology special publication number 6, p 28
10. EPA method 8031 (1994) Acrylonitrile by gas chromatography. Revision, September
11. Galíndez-Mayer J, Ramón-Gallegos J, Ruiz-Ordaz N, Juárez-Ramírez C, Salmerón-Alcocer A, Poggi-Varaldo HM (2008) Phenol and 4-chlorophenol biodegradation by yeast Candida tropicalis in a fluidized bed reactor. Biochem Eng J 38:147–157. doi:10.1016/j.bej.2007.06.011

12. Harper BD (1977) Microbial metabolism of aromatic nitriles. Biochem J 165:309–319
13. Jin Y, Veiga CM, Kennes C (2006) Performance optimization of the fungal biodegradation of α-pinene in gas-phase biofilter. Process Biochem 41:1722–1728. doi:10.1016/j.procbio.2006.03.020
14. Kennes C, Veiga MC (eds) (2001) Bioreactors for waste gas treatment. Ser Environ Pollut 4:112–114
15. Klecka GM, McDaniel SG, Wilson PS, Carpenter CL, Clarck JE, Thomas A, Spain JC (1996) Field-evaluation of a granular activated carbon fluid-bed bioreactor for treatment of chlorobenzene in groundwater. Environ Prog 15:93–107. doi:10.1002/ep.670150212
16. Mendoza JA, Prado OJ, Veiga MC, Kennes C (2004) Hydrodynamic behaviour and comparison of technologies for the removal of excess biomass in gas-phase biofilters. Water Res 38:404–413. doi:10.1016/j.watres.2003.09.014
17. Nagasawa T, Mathew CD, Mauger J, Yamada H (1988) Nitrile hydratase catalysed production of niconamide from 3-cyanopyridine in *Rhodococcus rhodochrous* J1. Appl Environ Microbiol 54:1766–1769
18. Nagasawa T, Yamada H (1990) Application of nitrile converting enzymes for the production of useful compounds. Pure Appl Chem 62:1441–1444. doi:10.1351/pac199062071441
19. Oh YS, Bartha R (1994) Design and performance of a trickling air biofilter for clorobenzene and o-diclorobenzene vapors. Appl Environ Microbiol 60:2717–2722
20. Sa CSA, Bonaventura RAR (2001) Biodegradation of phenol by *Pseudomonas putida* DSM 548 in a trickling bed reactor. Biochem Eng J 9:211–219. doi:10.1016/S1369-703X(01)00149-8
21. Shi J, Zhao XD, Hichey RF, Voice TC (1995) Role of adsorption in granular activated carbon-fluidized bed reactors. Water Environ Res 67:302–309. doi:10.2175/106143095X131510
22. Stanier RY, Palleroni NJ, Doudoroff M (1966) The aerobic pseudomonads: a taxonomic study. J Gen Microbiol 43:159–271
23. U.S.EPA (1985) U.S. Environmental Protection Agency. Health and Environmental Effects Profile for Acrylonitrile. Environmental Criteria and Assessment Office, U.S, EPA, Cincinnati, OH
24. U.S.EPA (1992) The Clean Air Act Amendments of 1990: A guide for small business
25. U.S.EPA (1994) U.S. Environmental Protection Agency. Integrated Risk Information System(IRIS) Database. Reference concentration (RfC) for acrylonitrile. Available online at http://www.epa.gov/iris/subst/0206.htm
26. U.S.EPA (2003) National Emission Standards for Hazardous Air Pollutants: Miscellaneous Organic Chemical Manufacturing. November 10, 2003 (Volume 68, Number 217)
27. Watanable I, Yoshiaki S, Enomoto K (1987) Screening, isolation and taxonomical properties of microorganisms having acrylonitrile-hydrating activity. Agric Biol Chem 51:3193–3199
28. Weissermel K, Arpe HJ (1997) Industrial organic chemistry. 3rd Revised edn. VCH Publishers Inc, New York, pp 302–310
29. Wyatt JM, Knowles CJ (1995) The development of a novel strategy for the microbial treatment of acrylonitrile effluents. Biodegradation 6:93–107. doi:10.1007/BF00695340
30. Xing J, Hickey R (1994) Response in performance of the GAF-fludized bed reactor process for BTX removal to perturbation in oxygen and nutrient supply. Int Biodeter Biodegrad 33:23–39. doi:10.1016/0964-8305(94)90053-1
31. Xu DX, Zhu QX, Zheng LK, Wang QN, Shen HM, Deng LX, Ong CN (2003) Exposure to acrylonitrile induced DNA strand breakage and sex chromosome aneuploidy in human spermatozoa. Mutat Res Genet Toxicol Environ Mutagen 537:93–100. doi:10.1016/S1383-5718(03)00055-X
32. Zhou Q, Huang YL, Tseng DH, Shim H, Yang ST (1998) A trickling fibrous-bed bioreactor for biofiltration of benzene in air. J Chem Technol Biotechnol 73:359–368. doi:10.1002/(SICI)1097-4660(199812)73:4<359::AID-JCTB970>3.0.CO;2-V